Micro Wind Power Generator with Battery Energy Storage for Critical Load

Sharad W. Mohod, *Member, IEEE,* and Mohan V. Aware

***Abstract*—In the micro-grid network, it is especially difficult to support the critical load without uninterrupted power supply. The proposed micro-wind energy conversion system with battery energy storage is used to exchange the controllable real and reactive power in the grid and to maintain the power quality norms as per International Electro-Technical Commission IEC-61400-21 at the point of common coupling. The generated micro-wind power can be extracted under varying wind speed and can be stored in the batteries at low power demand hours. In this scheme, inverter control is executed with hysteresis current control mode to achieve the faster dynamic switchover for the support of critical load. The combination of battery storage with micro-wind energy generation system (μWEGS), which will synthesize the output waveform by injecting or absorbing reactive power and enable the real power flow required by the load. The system reduces the burden on the conventional source and utilizes μWEGS and battery storage power under critical load constraints. The system provides rapid response to support the critical loads. The scheme can also be operated as a stand-alone system in case of grid failure like a uninterrupted power supply. The system is simulated in MATLAB/SIMULINK and results are presented.**

***Index Terms*—Battery energy storage, micro-wind energy generating system, power quality.**

I. Introduction

WITH HIGH population growth and economic development in the world, there is a very high demand for energy. Traditional fossil sources such as oil, coal are costly and have a serious pollution to the environment. As a renewable energy, wind energy generation has been focused as a clean and inexhaustible energy providing a feasible solution to energy shortage. The micro wind power generation system with battery energy storage is becoming more prominent with the increasing demand of power generation. It also reduces the environment pollution. However the output power of micro-wind generator is fluctuating and will affect the operation in the distribution network. The utility system cannot accept new generation without strict condition of voltage regulation due to real power fluctuation and reactive power generation/absorption. The industrial and commercial customers often operate the sensitive electronic equipments or critical load that cannot tolerate voltage sags, voltage swells, or loss of power, which moreover cause interruption in life operating equipments or stoppage in industrial production. This requires some measure to mitigate the output fluctuation so as to keep the power quality in the distributed network. International Electro-Technical Commission IEC-61400-21 describes the norms for power quality of micro-wind generating system. The battery storage is used for critical load applications as it supplies power for a short period of time. The combination of battery energy storage and micro-wind generating system in distributed power system can provide the effective, reliable, and durable power system. The system also provides energy saving and un-interruptible power within distribution network [1]–[3]. In Japan, battery energy storage was used for mitigation of variations in wind farm output to stabilize the short fluctuation of output power [4]. The parallel processing of wind energy generating system and battery storage will enhance the power flow in the distributed network. The micro-wind energy generating system is used to charge the battery as and when the wind power is available. The control method for the state of charge of battery unit was proposed in [5]. The battery storage provides a rapid response for either charging/discharging the battery and also acts as a constant voltage source for the critical load in the distributed network. The battery storage system utilizes flooded lead-acid battery cell for energy storage. For electrical energy storage application, a large number of cells are connected in series to produce the required operating voltage [6], [7]. In order to verify the effectiveness of proposed system, the current control mode of voltage source inverter is proposed to interface the battery storage with micro-wind energy generator into the distributed network. The proposed control system with battery storage has the following objectives:

1) unity power factor and power quality at the point of common coupling bus;
2) real and reactive power support from wind generator and batteries to the load;
3) stand-alone operation in case of grid failure.

This paper is organized as follows. Section II introduces the wind power extraction with batteries, Section III introduces the control scheme, Section IV describes the system performance,

Manuscript received September 17, 2010; revised February 10, 2011; accepted May 25, 2011. Date of publication August 30, 2011; date of current version February 23, 2012.

S. W. Mohod is with the Department of Electronic Engineering, Prof. Ram Meghe Institute of Technology and Research, Badnera, Amravati 444701, India, and also with the Visvesvaraya National Institute of Technology, Nagpur 440011, India (e-mail: sharadmohod@rediffmail.com).

M. V. Aware is with the Department of Electrical Engineering, Visvesvaraya National Institute of Technology, Nagpur 440011, India (e-mail: mva_win@yahoo.com).

Color versions of one or more of the figures in this paper are available online at http://ieeexplore.ieee.org.

Digital Object Identifier 10.1109/JSYST.2011.2163015

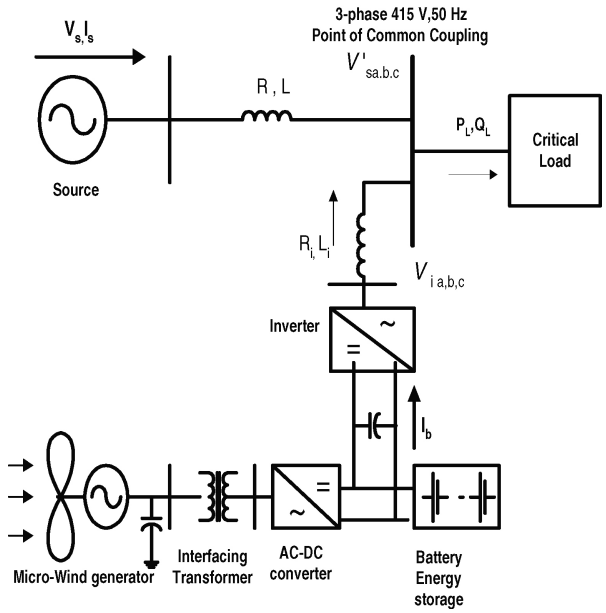

Fig. 1. Scheme of micro-wind generator with battery storage for critical load application.

and Sections V and VI describe the experimental results and conclusion.

II. Wind Power Extraction with Batteries

The proposed micro-wind energy extraction from wind generator and battery energy storage with distributed network is configured on its operating principle and is based on the control strategy for switching the inverter for critical load application as shown in Fig. 1.

A. Micro-Wind Energy Generating System

The micro-wind generating system (μWEGS) is connected with turbine, induction generator, interfacing transformer, and ac-dc converter to get dc bus voltage. The power flow is represented with dc bus current for constant dc bus voltage in inverter operation.

The static characteristic of wind turbine can be described with the relationship in the wind as in

$$P_{\text{wind}} = \frac{1}{2}\rho \Pi R^2 V_{\text{wind}}^3 \tag{1}$$

where ρ is air density ($1.225\,\text{kg/m}^3$), R is the rotor radius in meters, and V_{wind} is the wind speed in m/s. It is not possible to extract all kinetic energy of wind and is called C_P power coefficient. This power coefficient can be expressed as a function of tip speed ratio λ and pitch angle θ. The mechanical power can be written as (2)

$$P_{\text{mech}} = C_p P_{\text{wind}} \tag{2}$$

$$P_{\text{mech}} = \frac{1}{2}\rho \Pi R^2 V_{\text{wind}}^3 C_p. \tag{3}$$

By using the turbine rotational speed, ω_{turbine} mechanical-torque is shown in

$$T_{\text{mech}} = P_{\text{mech}}/\omega_{\text{turbine}}. \tag{4}$$

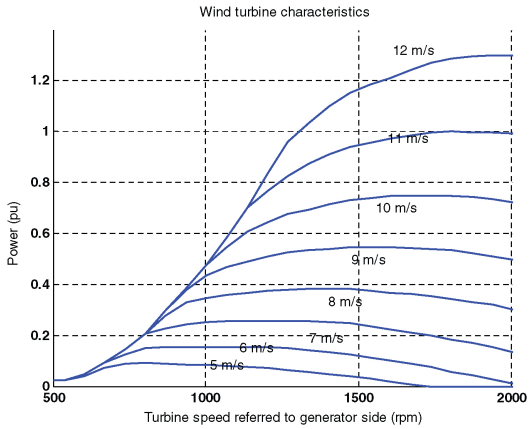

Fig. 2. Power-speed characteristic of turbine.

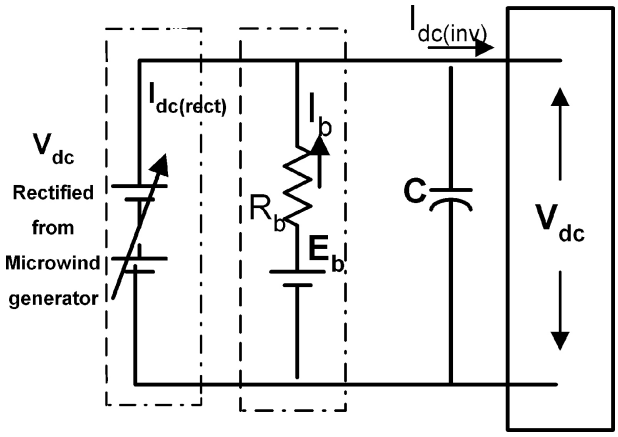

Fig. 3. Dc link for battery storage and micro-wind generator.

The speed-power characteristic of variable speed wind turbine is given in Fig. 2.

B. Dc Link for Battery Storage and Micro-Wind Energy Generator

The battery storage and μWEGS are connected across the dc link as shown in Fig. 3. The dc link consists of capacitor which decouples the μwind generating system and ac source (grid) system [8], [9]. The battery storage will get charged with the help of μwind generator. The use of capacitor in dc link is more efficient, less expensive and is modeled as follows:

$$C\frac{d}{dt}V_{\text{dc}} = I_{\text{dc(rect)}} - I_{\text{dc(inv)}} - I_b \tag{5}$$

where C is dc link capacitance, V_{dc} is rectifier voltage, $I_{\text{dc(rect)}}$ is rectified dc-side current, $I_{\text{dc(inv)}}$ is inverter dc-side current, and I_b is the battery current.

The battery storage is connected to dc link and is represented by a voltage source E_b connected in series with an internal resistance R_b. The internal voltage varies with the charged status of the battery. The terminal voltage V_{dc} is given in

$$V_{\text{dc}} = E_b - I_b * R_b \tag{6}$$

where I_b represents the battery current.

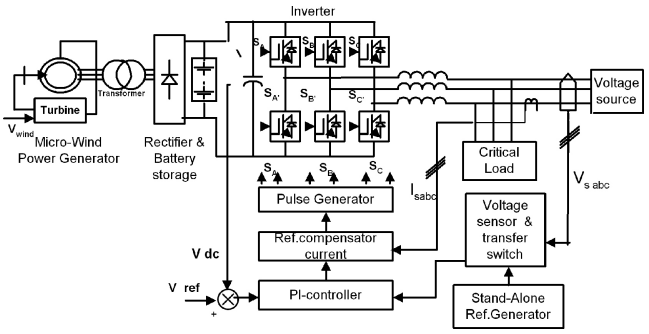

Fig. 4. Inverter interface with combination of battery storage with μWEGS.

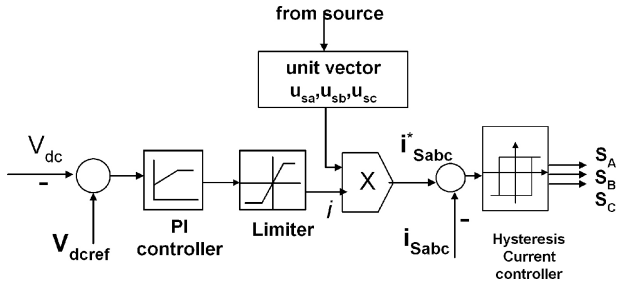

Fig. 5. Control scheme for switching the inverter circuit.

It is necessary to keep adequate dc link level to meet the inverter voltage [10] as in

$$V_{\rm dc} \geq \frac{2\sqrt{2}}{M_a} V_{\rm inv} \tag{7}$$

where $V_{\rm inv}$ is the line-to-neutral rms voltage of inverter (240 Vrms), inverter output frequency 50 Hz, and M_a is modulation index (9). Thus, the dc link is designed for 800 V.

III. Control Scheme of the System

The control scheme with battery storage and micro-wind generating system utilizes the dc link to extract the energy from the wind. The micro-wind generator is connected through a step up transformer and to the rectifier bridge so as to obtain the dc bus voltage. The battery is used for maintaining the dc bus voltage constant; therefore the inverter is implemented successfully in the distributed system [11]–[13]. The three-leg 6-pulse inverter is interfaced in distributed network and dual combination of battery storage with micro-wind generator for critical load application, as shown in Fig. 4.

The control scheme approach is based on injecting the current into the grid using "hysteresis current controller." Using such techniques the controller keeps the control system variables between the boundaries of hysteresis area and gives correct switching signals for inverter operation.

The control scheme for generating the switching signals to the inverter is shown in Fig. 5.

The control algorithm needs the measurement of several variables such as three-phase source current $i_{\rm Sabc}$ for phases a, b, c, respectively, dc voltage $V_{\rm dc}$, inverter current $i_{\rm iabc}$ with the help of sensors. The current control block receives an input of reference current $i^*_{\rm Sabc}$ and actual current $i_{\rm Sabc}$ is measured from source phase a, b, c, respectively, and are subtracted so as to activate the operation of the inverter in current control mode.

A. Grid Synchronization

In the three-phase balance system, the RMS voltage source amplitude is calculated at the sampling frequency from the source phase voltage ($V_{\rm sa}$, V_b, $V_{\rm sc}$) and is expressed as sample template $V_{\rm sm}$ [14], as in

$$V_{\rm sm} = \left\{ \frac{2}{3} \left(V_{\rm sa}^2 + V_{\rm sb}^2 + V_{\rm sc}^2 \right) \right\}^{1/2}. \tag{8}$$

The in-phase unit vectors are obtained from ac source-phase voltage and the RMS value of unit vector $u_{\rm sa}, u_{\rm sb}, u_{\rm sc}$ as shown in

$$u_{\rm sa} = \frac{V_{\rm Sa}}{V_{\rm sm}}, u_{\rm sb} = \frac{V_{\rm Sb}}{V_{\rm sm}}, u_{\rm sc} = \frac{V_{\rm Sc}}{V_{\rm sm}}. \tag{9}$$

The in-phase generated reference currents are derived using the in-phase unit voltage template as in

$$i^*_{\rm sa} = i.u_{\rm sa}, i^*_{\rm sb} = i.u_{\rm sb}, i^*_{\rm sc} = i.u_{\rm sc} \tag{10}$$

where i is proportional to the magnitude of filtered source voltage for respective phases. It is the output taken from proportional-integral controller. This ensures that the source current is controlled to be sinusoidal. The unit vector implements the important function in the grid for the synchronization of inverter. This method is simple, robust and favorable as compared with other methods.

When the grid voltage source fails the micro-wind generator acts as a stand-alone generator. Under such conditions the voltage sensors sense the condition and will transfer the micro-switches for the generation of reference voltage from micro-wind generator. The above generated reference under no source supply gets switched to the stand-alone reference generator after voltage sensing at the point of common coupling. This is a unit voltage vector which can be realized by using microcontroller or DSP. Thus, the inverter maintains the continuous power for the critical load.

B. Hysteresis Based Current Controller

Hysteresis based current controller is implemented in the current control scheme. The reference current is generated as in (10) and the actual current is detected by current sensors that are subtracted for obtaining current errors for a hysteresis based controller. The ON/OFF switching signals for IGBT of inverter are derived from hysteresis controller. When the actual (measured) current is higher than the reference current, it is necessary to commutate the corresponding switch to get negative inverter output voltage. This output voltage decreases the output current and reaches the reference current. On the other hand, if the measured current is less than the reference current, the switch commutated to obtain a positive inverter output voltage. Thus the output current increases and it goes to the reference current. As a result, the output current will be within a band around the reference one. The switching function S_A for phase a is expressed as follows:

$$i_{\rm sa} > (i^*_{\rm sa} + HB) \rightarrow S_A = 1$$

$$i_{\rm sa} < (i^*_{\rm sa} - HB) \rightarrow S_A = 0 \tag{11}$$

TABLE I
SYSTEM PARAMETERS

Source voltage	3-phase, 415 V, 50 Hz
Source and line inductance	0.5 mH
Micro-wind generator parameter (induction generator)	150 kW, 415 V, 50 Hz, $P = 4$, Rs = 0.01 Ω, Rr = 0.015 Ω, Ls = 0.06 H, Lr = 0.06 H, wind velocity 5 m/s
DC link parameter	DC link-800 V, $C = 5\ \mu$F
Rectifier-bridge parameter (three arm bridge type)	Snubber $R = 100\ \Omega$, Ron = 0.01 Ω, snubber capacitance = 0.01e-3 F
IGBT device parameters (three arm bridge type)	Rated voltage 1200 V, Forward.Current 50 A, gate voltage +/-20 V, turn-ON delay 70 ns, turn-OFF delay 400 ns, power dissipation 300 W
Battery parameters	DC 800 V, cell capacity 500 Ah, type-lead acid
Interfacing transformer	Rating-1 KVA, Y-Y type, 415/800 V, 50 Hz
Critical load parameter	3-phase 415 V, non-linear load $R = 10\ \Omega$, $C = 1\ \mu$F

where HB is a hysteresis current-band, similarly the switching function S_B, S_C can be derived for phases "b" and "c," respectively. The current control mode of inverter injects the current into the grid in such a way that the source currents are harmonic free and their phase-angles are in-phase with respect to source voltage. Thus, the injected current will cancel out the reactive and harmonic part of load current. Thus, it improves the source current quality at the PCC. The power transfer takes place as soon as battery energy system is fully charged with the help of micro-wind generator. To achieve this goal, the source voltage is sensed and synchronized in generating the desired reference current command for the inverter operation.

The implementation of the hysteresis band current control is not expensive. The control is excellent for a fast response of an inverter to rapid changes of reference current, since current control has negligible inertia and delay.

IV. SYSTEM PERFORMANCE

The scheme of micro-wind generator with battery energy storage for extraction of wind energy for critical load application is shown in Fig. 1 and is simulated in MATLAB/SIMULINK with power system block set. A simulink model library includes the model of converter, induction generator, critical load, and others that has been constructed for simulation [15]–[19].

The simulation parameters for the given system are given in Table I.

A. Dynamic Performance Under Power Quality Mode

A critical load is considered as a nonlinear load for the simulation of the system. The performance of the system is observed for the power quality improvement of critical load. The inverter is switched "on" at 0.2 s. The source current I_s, inverter injected current I_{inv}, and load current I_L are measured with and without controller operation. The current supplied from the source is made sinusoidal, harmonics-free

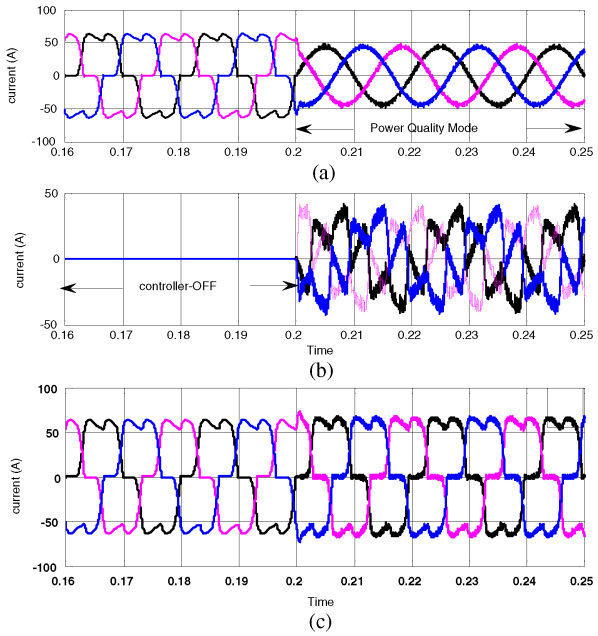

Fig. 6. (a) Source current. (b) Inverter injected current. (c) Load current.

as soon as controller is in operation and is shown in Fig. 6(a). The injected current supplied from the inverter is shown in Fig. 6(b). The critical load current in the system is shown in Fig. 6(c). During this interval, the load current will be the addition of source current and inverter current.

B. Dynamic Performance Under Stand-Alone Mode

It is observed that the system is operating in power quality mode up to 0.6 s. The dynamic performance of the system is monitored by operating the circuit breaker at 0.6 s. Under such condition the system performs as a stand-alone mode. The voltage sensor senses the condition and transfers the micro switches to generate the reference current in stand-alone reference generator. During this mode the inverter will support the critical load in the absence of source voltage. Due to the unavailability of source, the inverter will supply the full load current in this duration. The source current, load current, and inverter current in stand-alone mode are shown in Fig. 7.

C. Dc Link Performance for Micro-Wind Generator and Battery Storage

The micro-wind energy generator is operated to generate the power and is supplied to uncontrolled rectifier to interface the dc link. The battery model is considered as it gets charged separately so as to take the advantage of wind source. This coordination is made manually in the simulation of the system. The dc link voltage is shown in Fig. 8(a). To transfer the real power from wind generator into the load, the generated power is fed to rectifier for charging the batteries. The rectified current from wind generator is shown in Fig. 8(b) and current supplied from battery storage is shown in Fig. 8(c). At 0.6 s the system is operated as a stand-alone mode, during this situation only storage battery supports the critical load. The charging and discharging of dc link capacitor is shown in Fig. 8(d).

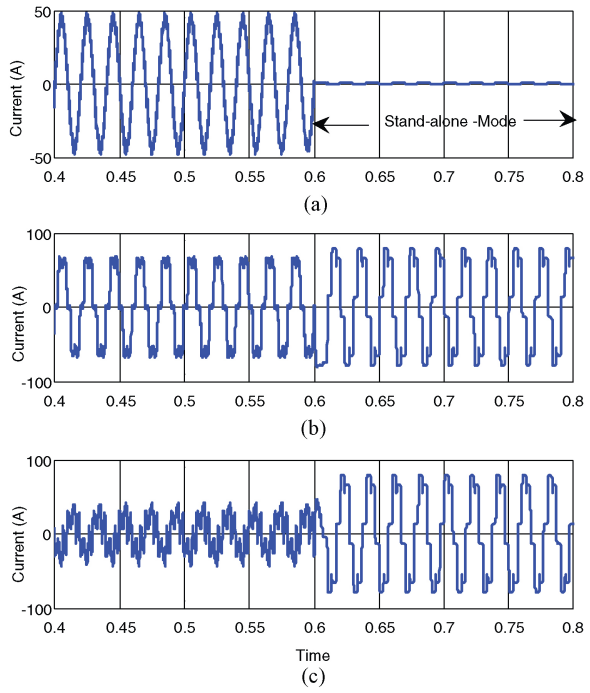

Fig. 7. (a) Source current. (b) Load current. (c) Inverter-injected current.

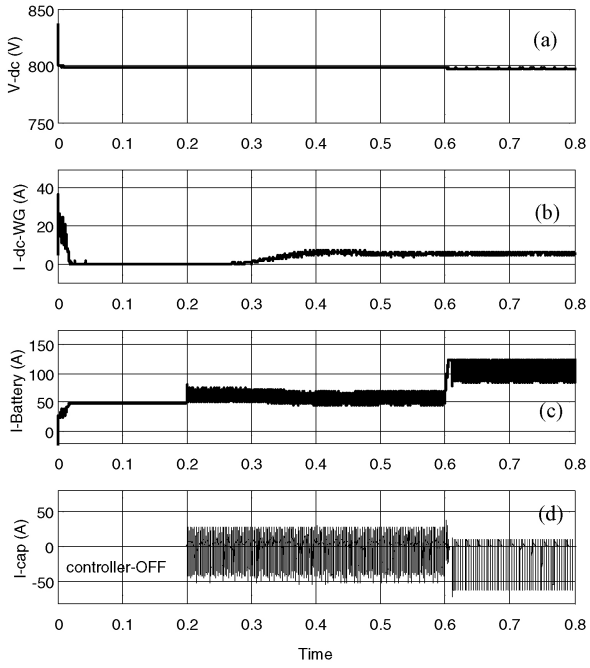

Fig. 8. (a) DC link voltage. (b) Rectified current of wind generator. (c) Current supplied by battery. (d) Charging-discharging of dc link capacitor.

D. Performance of PI Controller

The proportional-integral type controller is used in the control system and its response is very fast. It corrects the error between measured variable and a desired set value. The K_p determine amplification to the current error and K_i process the corrected error. The PI controller used to increase the overshoot increases the change in the settling time and eliminates the steady state error in the system. The increase in

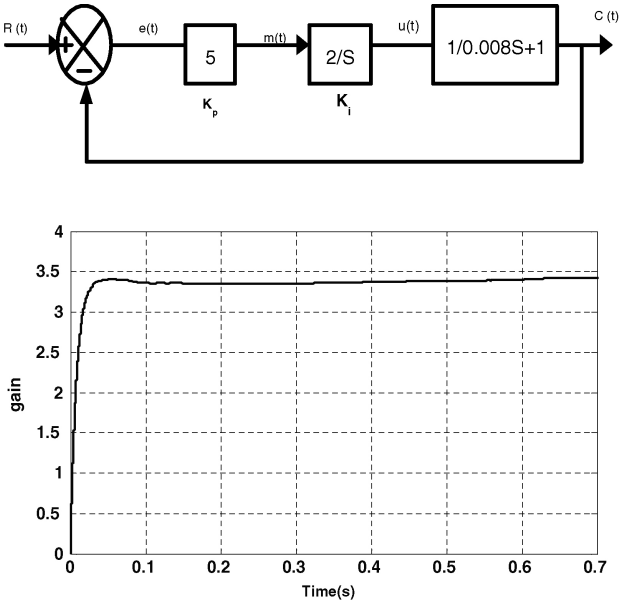

Fig. 9. (a) Realization of transfer function. (b) Controller performance.

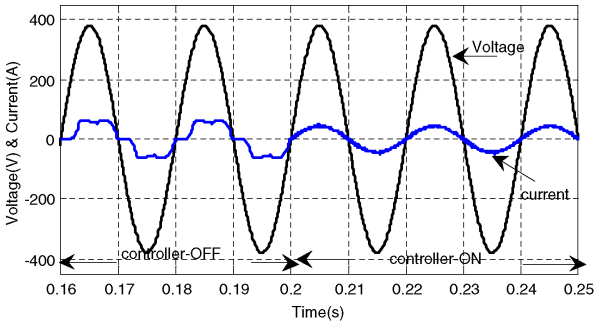

Fig. 10. Source current and source voltage at PCC.

the loop gain K_p improves the steady state tracking accuracy, disturbance signal rejection, the relative stability and also makes the system less sensitive to the parameter variations. The integral controller reduces the steady state error without the need for manual reset. The transfer function for the simulation is considered as in

$$G(s) = \frac{10}{0.008s + 1}. \tag{12}$$

The realization of (12) is shown in Fig. 9(a) and the performance of controller is shown in Fig. 9(b).

The performance of controller is used to stabilize the voltage in the distributed network. The source current is maintained in phase with the source voltage, indicating the unity power factor at point of common coupling and satisfies power quality norms. The results of in-phase source current and source voltage are shown in Fig. 10.

The current waveform before and after the inverter operation is analyzed for power quality measures. The Fourier analysis of the waveform is expressed without the inverter-controller in the system and the THD of the source current signal is shown in Fig. 11(a), the measured THD and its harmonics order is shown in Fig. 11(b).

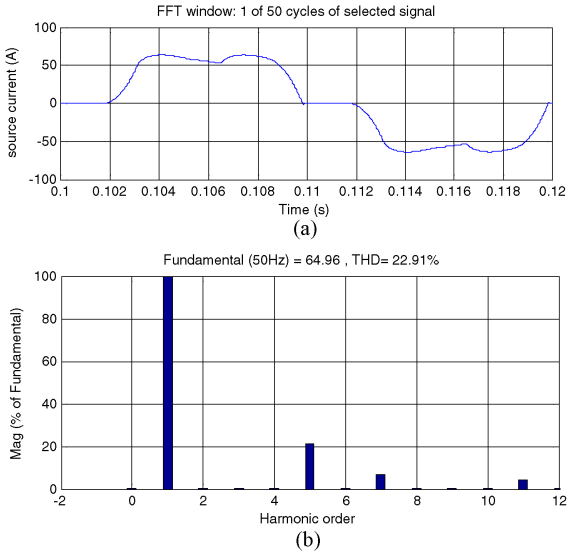

Fig. 11. (a) Source current. (b) FFT of source current.

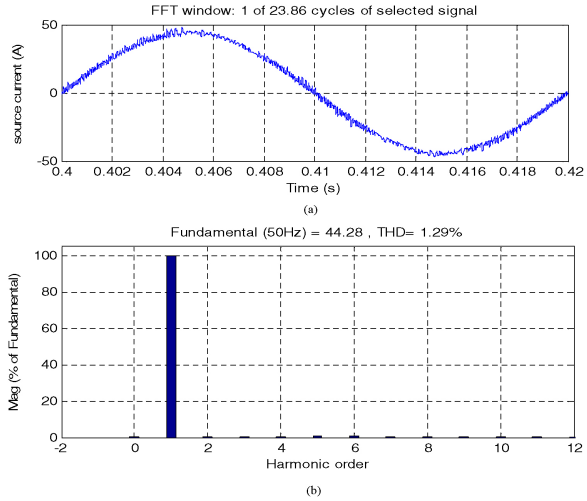

Fig. 12. (a) Source current. (b) FFT of source current.

TABLE II
PERFORMANCE OF CONTROLLER OPERATION

Harmonics order in source current	F	3	5	7	9	11	THD
Without controller	64.9	0.1	22	10	0.1	8	22.9
With controller	44.2	0.2	0.6	0.2	0.1	0.35	1.29
With International Electro-Technical Standard							3.0

The power quality improvement is observed at the point of common coupling, when the controller is in ON condition. The inverter is placed in the operation and source current waveform is shown in Fig. 12(a), with its FFT in Fig. 12(b). It is shown that the THD has been improved considerably and within the norms of its standard. The comparative performance with and without inverter controller and international electro-technical standard is presented in Table II.

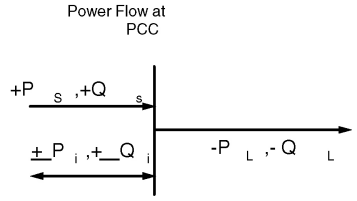

Fig. 13. Active and reactive power flow at PCC.

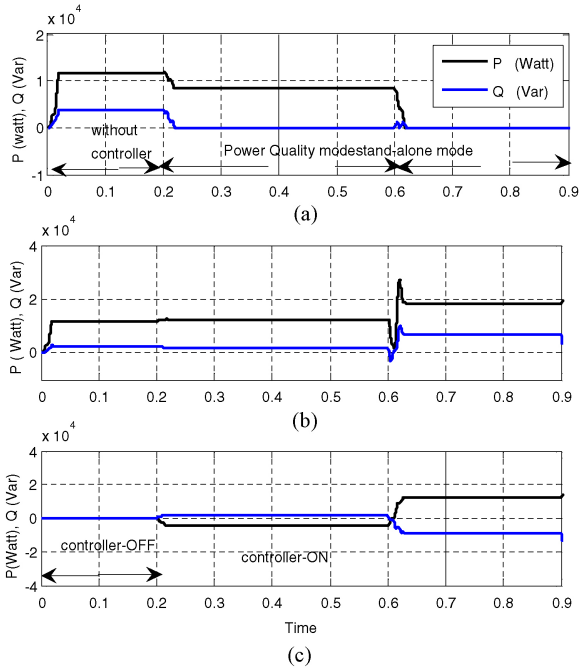

Fig. 14. Active and reactive power (a) at source, (b) load, and (c) inverter.

E. Active and Reactive Power Flow at PCC in Micro-Grid

The average power flow for the proposed system can be monitored on PCC for active and reactive power flow (P_S, Q_S) of the source, inverter power (P_i, Q_i) and the load (P_L, Q_L) is shown in Fig. 13.

The average power flow is measured at the point of common coupling, with and without controller operation in the grid. The controller is operated for power quality mode to inject the power at $t = 0.2$ s, during this operation source reactive power is reduced to zero, as it is supported from the inverter during power quality mode. The micro-wind generator is operated as a stand-alone mode at $t = 0.6$ s, during this mode the source current is zero. In this mode only the inverter will support the demanded active and reactive power-support for the critical load and line losses as the grid supply is not available in such mode of operation as shown in Fig. 14.

The above scheme for critical load application has not only power quality improvement but it also supports the critical load with the energy storage through the batteries.

V. EXPERIMENTAL RESULTS OF THE CONTROLLER

In order to validate the viability of the control scheme for switching the inverter, a laboratory prototype of the system is designed and fabricated.

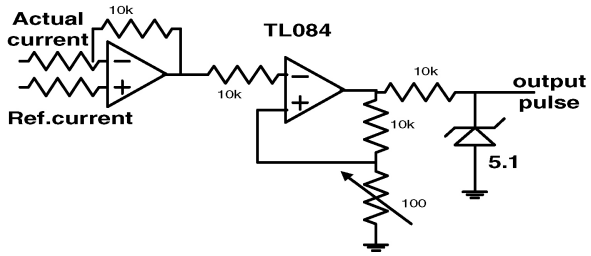

Fig. 15. Hysteresis controller.

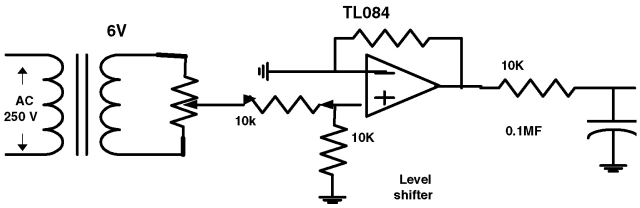

Fig. 16. Reference signal generator.

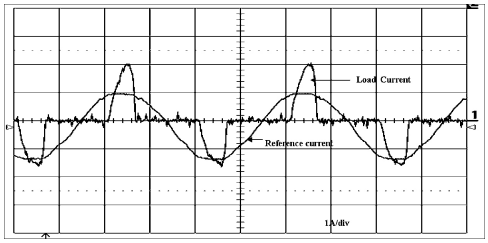

Fig. 17. Generated reference and load current.

A. Hysteresis Band Controller

The hysteresis band current controller circuit is developed as shown in Fig. 15. The reference and actual currents are the input to this circuit. These currents are compared within a hysteresis band which can be adjusted by potentiometer. The output of this controller is given to the delay circuit through opto-coupler and wave shaping circuits.

B. Reference Signal Generation Circuit

An ac voltage sensing circuit is required as an input for the hysteresis band current controller. The voltage magnitude is reduced by a step-down transformer. The signal magnitude can be reduced further by potential divider. A low-pass filter is inserted in this circuit and it serves as an anti-aliasing filter as shown in Fig. 16.

The output of the hysteresis band current controller is used as the input clock to this circuit. IC 74123 is used to generate the time delay. IC 74123 has a multivibrator feature and the pulse duration is controlled by the selection of external resistance and capacitor values.

The simple circuit of IC7404 as Schmitt-trigger is used to introduce any desired amount of dead band time between alternating output pulses.

The input signal to hysteresis current controller is reference current and non-sinusoidal load current as shown in Fig. 17.

For inverter circuit it is necessary to set an off timing "delay" (dead time) in order to prevent short circuits. During

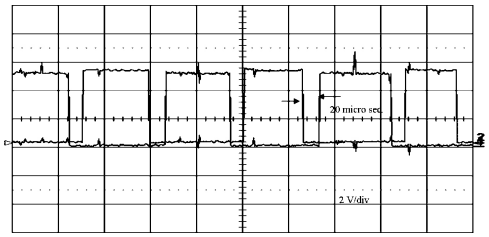

Fig. 18. Switching pulses for inverters.

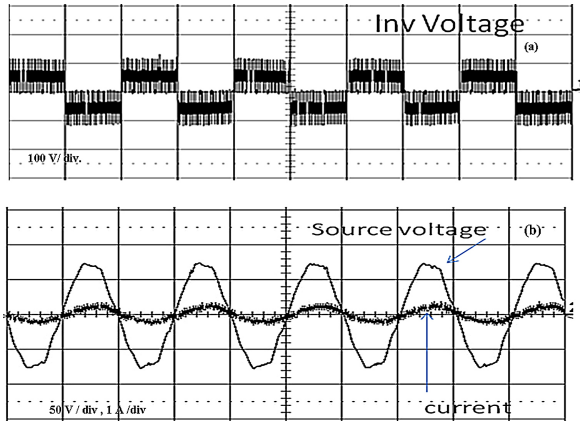

Fig. 19. (a) Inverter output voltage. (b) In-phase source voltage and current.

the dead time, both the upper and lower arms are in the "off" state. The dead time needs to be set longer than the IGBT switching time (t-off max). Dead time period must be suitable to avoid the problems of damaging the switches and associate harmonic problem. The switching pulses are generated for the inverter with dead band shown in Fig. 18.

The inverter is implemented in three pole arrangements with IGBT switches. The inverter output phase voltage as shown in Fig. 19(a) and the in-phase source voltage and source current at common point is shown in Fig. 19(b). It indicates that the proposed system is able to deliver the power to the grid with a unity power factor and low harmonics.

VI. Conclusion

The paper proposed micro-wind energy conversion scheme with battery energy storage, with an interface of inverter in current controlled mode for exchange of real and reactive power support to the critical load. The hysteresis current controller is used to generate the switching signal for inverter in such a way that it will cancel the harmonic current in the system. The scheme maintains unity power factor and also harmonic free source current at the point of common connection in the distributed network. The exchange of wind power is regulated across the dc bus having energy storage and is made available under the steady state condition. This also allows the real power flow during the instantaneous demand of the load. The suggested control system is suited for rapid injection or absorption of reactive/real power flow in the power system. The battery energy storage provides rapid response and enhances the performance under the fluctuation of wind turbine output and improves the voltage stability of

the system. This scheme is providing a choice to select the most economical real power for the load amongst the available wind-battery-conventional resources and the system operates in power quality mode as well as in a stand-alone mode.

REFERENCES

[1] D. Graovac, V. A. Katic, and A. Rufer, "Power quality problems compensation with universal power quality conditioning system," *IEEE Trans. Power Delivery*, vol. 22, no. 2, pp. 968–997, Apr. 2007.

[2] Z. Chen and E. Spooner, "Grid power quality with variable speed wind turbines," *IEEE Trans. Energy Conversion*, vol. 16, no. 2, pp. 148–154, Jun. 2008.

[3] Z. Yang, C. Shen, and L. Zhang, "Integration of stat COM and battery energy storage," *IEEE Trans. Power Syst.*, vol. 16, no. 2, pp. 254–262, May 2001.

[4] K. Yoshimoto, T. Nanahara, and G. Koshimizu, "Analysis of data obtained in demonstration test about battery energy storage system to mitigate output fluctuation of wind farm," in *Proc. CIGREE*, Jul. 2009, p. 1.

[5] L. Maharjan, S. Inoue, H. Akagi, and J. Asakur, "State-of-charge (SoC)-balancing control of a battery energy storage system based on a cascade PWM converter," *IEEE Trans. Power Electron*, vol. 24, no. 6, pp. 1628–1636, Jun. 2009.

[6] P. C. Loh, M. J. Newman, D. N. Zmood, and D. G. Holmes, "A comparative analysis of a multiloop voltage regulation strategies for single and three phase UPS system," *IEEE Trans. Power Electron*, vol. 18, no. 5, pp. 1176–1185, Sep. 2003.

[7] Z. Jiang, "Adaptive control strategy for active power sharing in hybrid fuel cell/battery power source," *IEEE Trans. Energy Conversion*, vol. 22, no. 2, pp. 507–515, Jun. 2007.

[8] B. S. Borowy and Z. M. Salameh, "Dynamic response of a stand-alone wind energy conversion system with battery energy storage to a wind gust," *IEEE Trans. Energy Conversion*, vol. 12, no. 1, pp. 73–78, Mar. 1997.

[9] P. F. Ribeiro, B. K. Johnson, M. L. Crow, A. Arsoy, and Y. Liu, "Energy storage system for advance power applications," *Proc. IEEE*, vol. 89, no. 12, pp. 1744–1756, Dec. 2001.

[10] B. Singh, S. S. Murthy, and S. Gupta, "Analysis and design of STATCOM-based voltage regulator for self-excited induction generator," *IEEE Trans. Energy Conversion*, vol. 19, no. 4, pp. 783–791, Dec. 2004.

[11] S. Teleke, M. E. Baran, A. Q. Huang, S. Bhattacharya, and L. Anderson, "Control strategy for battery energy storage for wind farms dispatching," *IEEE Trans Energy Conversion*, vol. 24, no. 3, pp. 725–731, Sep. 2009.

[12] N. M. Ahdel-Rahim and J. E. Quaicoe, "Analysis and design of a multiple feedback control strategy for a single-phase voltage-source ups inverter," *IEEE Trans. Power Electron*, vol. 11, no. 4, pp. 532–541, Jul. 2006.

[13] G. Tapia, "Proportional-integral regulator based application to wind farm reactive power management for secondary voltage control," *IEEE Trans. Energy Conversion*, vol. 22, no. 2, pp. 488–498, Jun. 2007.

[14] Y. Chauhan, S. Jain, and B. Sing, "Static volt-ampere reactive compensator for self-excited induction generator feeding dynamic load," *Electric Power Compon. Syst. J.*, vol. 36, no. 10, pp. 1080–1101, Oct. 2008.

[15] F. S. Pai and S.-I. Hung, "Design and operation of power converter for microturbine powered distributed generator with capacity expansion capability," *IEEE Trans. Energy Conversion*, vol. 3, no. 1, pp. 110–116, Mar. 2008.

[16] J. M. Carrasco, "Power-electronic system for grid integration of renewable energy source: A survey," *IEEE Trans. Ind. Electron.*, vol. 53, no. 4, pp. 1002–1014, Jun. 2006.

[17] S. W. Mohod and M. V. Aware, "Grid power quality with variable speed wind energy conversion," in *Proc. IEEE PEDES*, Dec. 2006, pp. 1–6.

[18] S. W. Mohod and M. V. Aware, "Power quality issues and its mitigation technique in wind energy conversion," in *Proc. IEEE ICQPH*, Sep.–Oct. 2008, pp. 1–6.

[19] S. W. Mohod and M. V. Aware, "A STATCOM-control scheme for grid connected wind energy system for power quality improvement," *IEEE Syst. J.*, vol. 2, no. 3, pp. 346–352, Sep. 2010.

[20] *MATLAB/SIMULINK User Guide*, MathWorks, Inc., Natick, MA, 1995.

Sharad W. Mohod (M'11) received the B.E. and M.E. degrees in electrical engineering from the Government College of Engineering, Aurangabad, India, in 1988 and 1992, respectively. Currently, he is pursuing the Ph.D. degree with the Visvesvaraya National Institute of Technology, Nagpur, India.

He was an Electrical Engineer with M/S Garware Polyester, Ltd., Aurangabad, from 1988 to 1991. In 1991, he joined the College of Engineering, Badnera, Amravati, India, and since 2006 has been an Associate Professor with the Department of Electronic Engineering, Prof. Ram Meghe Institute of Technology and Research, Badnera.

Mr. Mohod is currently a member of FIE (India), IETE, and LMISTE.

Mohan V. Aware received the B.E. and M.Tech. degrees in electrical engineering from the Government College of Engineering, Amravati, India, and the Indian Institute of Technology Bombay, Mumbai, India, in 1980 and 1982, respectively, and the Ph.D. degree from Nagpur University, Nagpur, India, in 2002 for his research work on DTC induction motor drives.

He has ten years of industrial experience with Crompton Greaves, Ltd., Nasik, India, and Nippon Denro Ispat, Ltd., Nagpur, Certified Energy Auditor. He was a Post-Doctoral Fellow with the Department of Electrical Engineering, Hong Kong Polytechnic University, Hung Hom, Kowloon, Hong Kong. He is currently a Professor with the Department of Electrical Engineering, Visvesvaraya National Institute of Technology, Nagpur.

Dr. Aware was a Commonwealth Fellow in the U.K.